UCRL-85579
PREPRINT

NUMERICAL SIMULATION OF THE BETA II EXPERIMENT

D. E. Shumaker
J. K. Boyd
B. McNamara
W. C. Turner

This paper was prepared for submittal to
American Physical Society Meeting
New York City
October, 12, 1981

October 1981

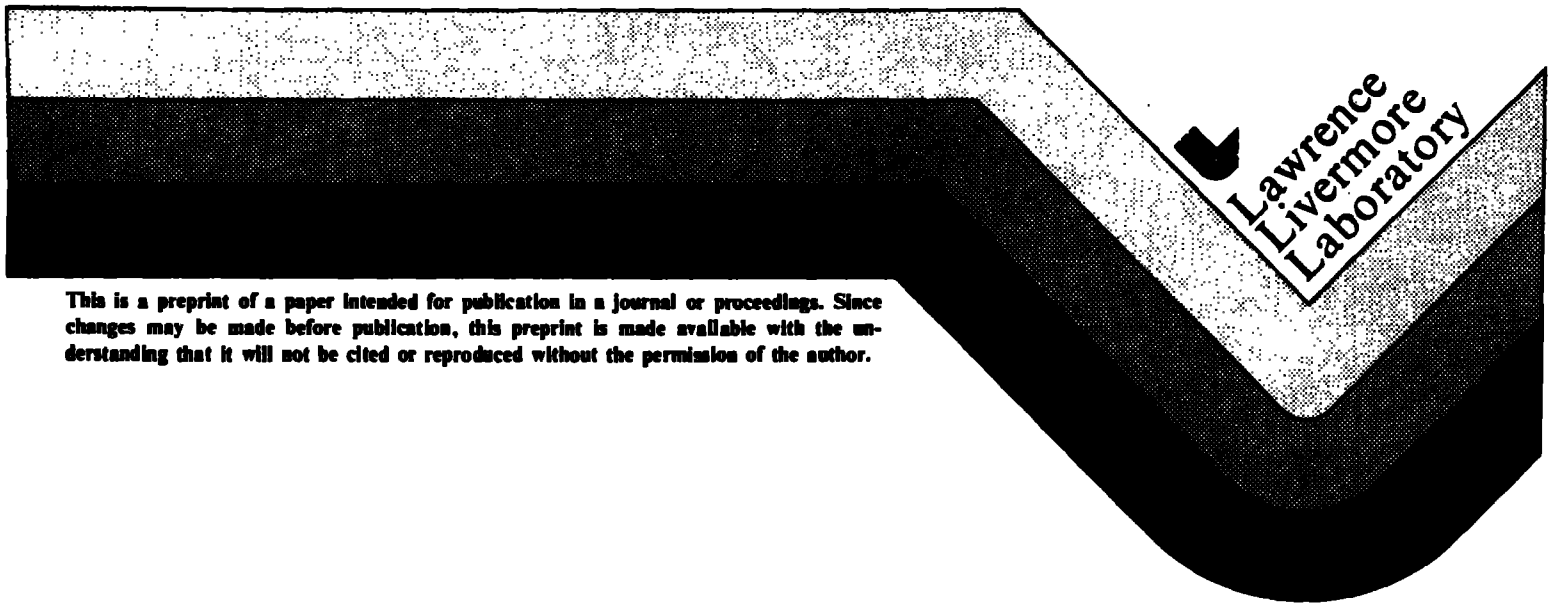

DISCLAIMER

Numerical Simulation of the Beta II Experiment*

D. E. Shumaker

National Magnetic Fusion Energy Computer Center

Lawrence Livermore National Laboratory

Livermore, California

J. K. Boyd, B. McNamara, W. C. Turner

Lawrence Livermore National Laboratory

Livermore, California

Abstract

The transport code FRT which is a 1-1/2-D transport-equilibrium code for an axisymmetric plasma was used to simulate the decay of the plasma and magnetic fields of the Beta II experiment. A comparison is made between the experimentally determined decay times for the magnetic fields and particle confinement times and the computed decay times. It is found that 1% oxygen impurity is enough to clamp the electron temperature below the radiation barrier, which is in agreement with the experiment.

---

*Work performed under the auspices of the U.S.D.O.E. by Lawrence Livermore National Laboratory under contract W-7405-ENG-48.

A. Description of the FRT Code

The FRT code [1] computes the evolution of an axisymmetric plasma on a transport time scale. The code alternates between the simultaneous solution of four 1-D transport equations and a 1-D or 2-D equilibrium calculation.

This code does not model the injection of the toroidal plasma into the flux conserver. The FRT code starts with the toroidal plasma in the flux conserver, and simulates its subsequent decay.

The transport code solves equations for the particle density, electron entropy, ion entropy and toroidal magnetic flux, using a normalized poloidal magnetic flux as an independent variable. The time rate of change of the poloidal magnetic flux enters the transport equations only through the normalizing constant, the flux at the 0-point. The poloidal flux at the 0-point is advanced from knowledge of the electric field at the 0-point. The transport coefficients used are the flux surface averaged Braginskii transport coefficients.

The electrons are heated by Joule heating and lose energy by impurity radiation and classical thermal conductivity multiplied by some constant (100 in this simulation).

The impurity species density is assumed to be given and is held constant during the calculation. The radiation cooling rate is computed using the data given in ref. (2), which assumes a coronal equilibrium.

The ions are heated by collisional transfer of energy from electrons, and lose energy by classical thermal conductivity.

The magnetic fluxes decay as a result of classical resistivity modified by Z_{eff} (effective ion charge) due to the impurities.

B. Results

The initial profiles of the electron and ion temperatures and ion density are shown in the first column of Fig. 1, as a function of r at z = 0. The initial profiles of the poloidal and toroidal magnetic fields are shown in the first column of Fig. 2. The initial poloidal flux between the separatrix and the 0-point is 3137 kG cm^2, and the initial toroidal flux enclosed by the separatrix is 1328 kG cm^2. The initial poloidal flux function is shown in Fig. 3. This simulation has a guide magnetic field of 100 G, which corresponds to a vacuum flux of 441.8 kG cm^2. The initial toroidal magnetic field at the 0-point was 2.7 kG, and at the end of the calculation, 175 μsec, the toroidal magnetic field at the 0-point was 0.75 kG. The initial poloidal magnetic field on the axis of rotational symmetry, (r = 0, z = 0), was -3.1 kG, at the end of the calculation it was -0.9 kG.

The initial electron and ion temperatures at the 0-point was 5eV. The initial ion density at the 0-point was 1.2×10^{15} cm^{-3}.

For this particular calculation the radiation cooling of the electrons assumes that the oxygen ion density is uniform across the plasma at a density of 1×10^{13} cm^{-3}.

There is an initial transient, approximately 10-20 μsec, during which time the Joule heating comes into balance with the impurity radiation cooling. During this transient the electron temperature adjusts itself to produce this balance. Fig. 4 is a plot of the electron and ion temperatures at the 0-point as a function of time. The electron and ion temperatures at the 0-point at the end of the transient is about 6.1 eV. The value of this temperature, for a given magnetic field, is determined mainly by two factors, (1) the initial ion density. A lower ion density yields a higher temperature at the end of the transient, due to there being more Joule heating energy per particle. Also the

radiation cooling is reduced for a lower ion density, (2) impurity ion density. A large impurity ion density will yield larger radiation loss and thus a lower electron temperature.

The ion temperature does not differ much from the electron temperature during this calculation due to the large collisional energy transfer rate.

The main power flow in this simulation is from the large reservoir of magnetic field energy to the electron via Joule heating. Fig. 5 is a plot of the Joule heating power and radiation cooling rate vs. time. The electron then loses the energy by radiation cooling. A small fraction of the Joule heating given to the electrons is transferred to the ions by collisions. The ions lose this energy by classical thermal conductivity. After the transient the electron temperature slowly drops due to the depletion of the magnetic field energy. The Joule heating rate and radiation cooling rate are approximately 20 M watts after the transient.

The time constant for the decay of the toroidal and poloidal magnetic fluxes are respectively 170 μsec, see Fig. 6. The decay is very nearly linear in time.

The total number of ions enclosed by the separatrix is nearly a constant in this calculation, Fig. 7. Also shown in Fig. 7 is the particle loss rate. The particle loss rate increases with time due mainly to the temperature dropping. The estimated particle confinement time from this data is 300 μsec.

Fig. 8 is a plot of β (plasma energy enclosed by separatrix/magnetic energy enclosed by separatrix). β increases in time due to the magnetic field decreasing. Also shown in Fig. 8 is the total toroidal current carried by the plasma. It decays approximately linearly with time. The discontinuities in this plot are where the 2-D equilibriums were computed.

Fig. 9 is the plot of the contours of the poloidal magnetic flux at the end of the calculation (175 μsec). Comparing to Fig. 3 the changes are slight. There has been some reduction in the volume enclosed by the separatrix. There has not been a significant shift in the 0-point.

In the Beta II experiment the magnetic field decay time was 110 μsec[3]. The decay time of the magnetic field in this calculation was 157 μsec for the poloidal magnetic flux and 166 μsec for the toroidal magnetic flux. The particle confinement time 500 μsec[3] compared to an estimated confinement time of 300 μsec for this calculation.

References

1. D. E. Shumaker, J. K. Boyd, S. P. Auerbach, and B. McNamara. "Numerical Simulation of Transport in a Field-Reversed Mirror Plasma" submitted to Journal of Computational Physics, UCRL-86566 (1981).

2. D. E. Post, R. V. Jensen, C. B. Tarter, W. H. Grasberger, and W. A. Lokke. "Steady State Radiation Cooling Rates for Low-Density High Temperature Plasmas," At. Data and Nucl. Data Tables (USA), Vol. 20, No. 5, p. 397 (1977).

3. W. C. Turner, G. C. Goldenbaum, E. H. A. Granneman, C. W. Hartman, D. S. Prono, J. Taska, and A. C. Smith, Jr. "Formation of Compact Toroidal Plasmas by Magnetized Coaxial Plasma Gun Injection into an Oblate Flux Conserver," Proceedings of the Third Symposium on The Physics and Technology of Compact Toroids in the Magnetic Fusion Energy Program," Los Alamos, NM, LA-8700-C (1980).

Figure Captions

Fig. 1. Profiles of electron temperature, T_e, ion temperature, T_i, and ion density, N_i, at various times. Profiles are plotted as a function of r at z = 0.

Fig. 2. Profiles of toroidal current density, J_θ, poloidal magnetic field, B_p, and toroidal magnetic field, B_t, at various times. Profiles are plotted as a function of r at z = 0.

Fig. 3. Contours of the initial poloidal magnetic flux function.

Fig. 4. Electron temperature, T_e, and ion temperature, T_i, at O-point vs. time.

Fig. 5. Total Joule heating and radiation cooling rates vs. time.

Fig. 6. Toroidal magnetic flux and poloidal magnetic flux vs. time.

Fig. 7. Number of particles enclosed by separatrix, and particle loss rate vs. time.

Fig. 8. β, (plasma energy enclosed by separatrix/magnetic energy enclosed by separatrix) and total toroidal current vs. time.

Fig. 9. Contours of the final poloidal magnetic flux function.

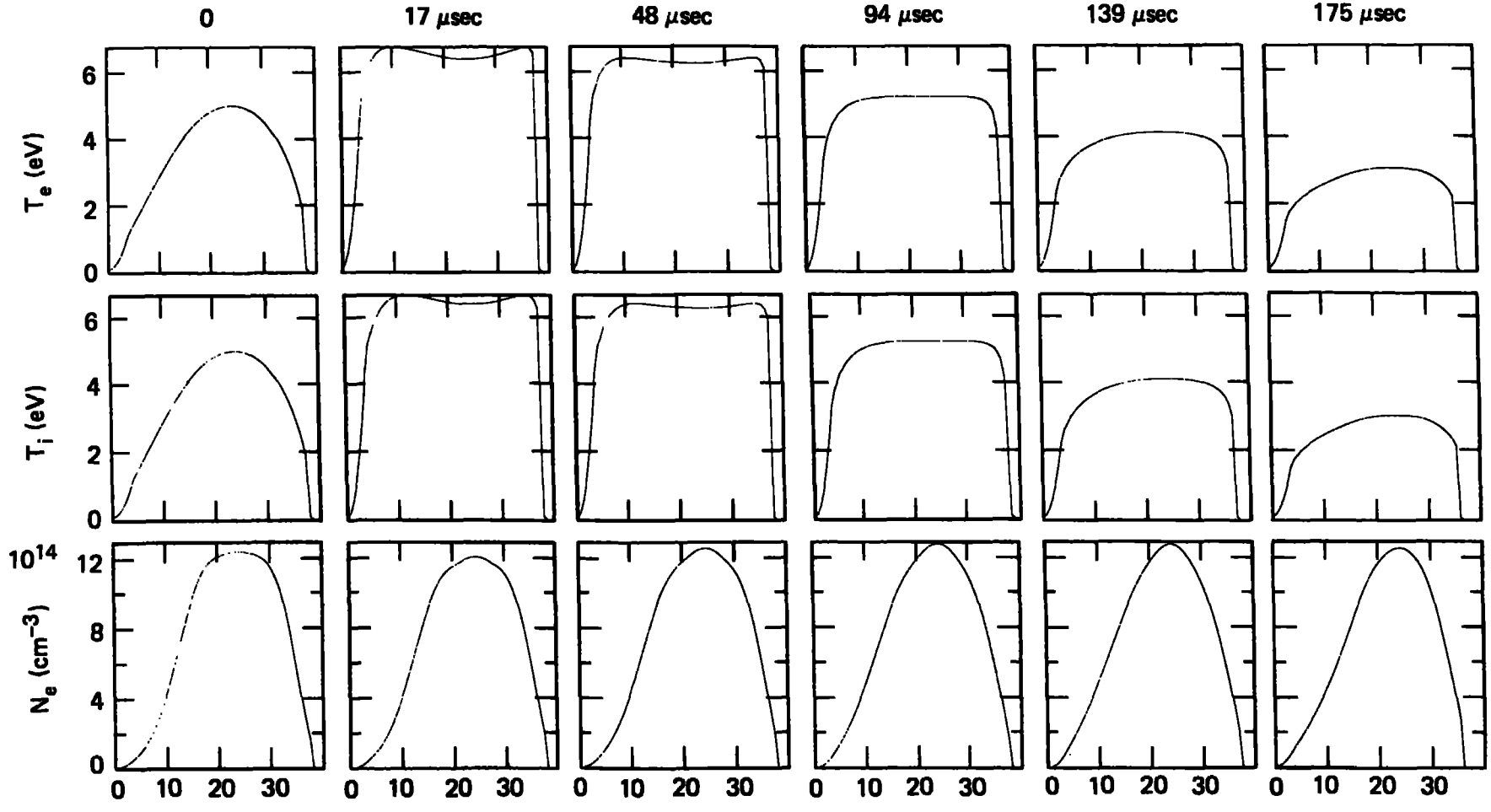
0
17 μsec
48 μsec
94 μsec
139 μsec
175 μsec
T_e (eV)
T_i (eV)
10^{14}
N_e (cm^{-3})
0
2
4
6
8
12
0 10 20 30

Figure 1

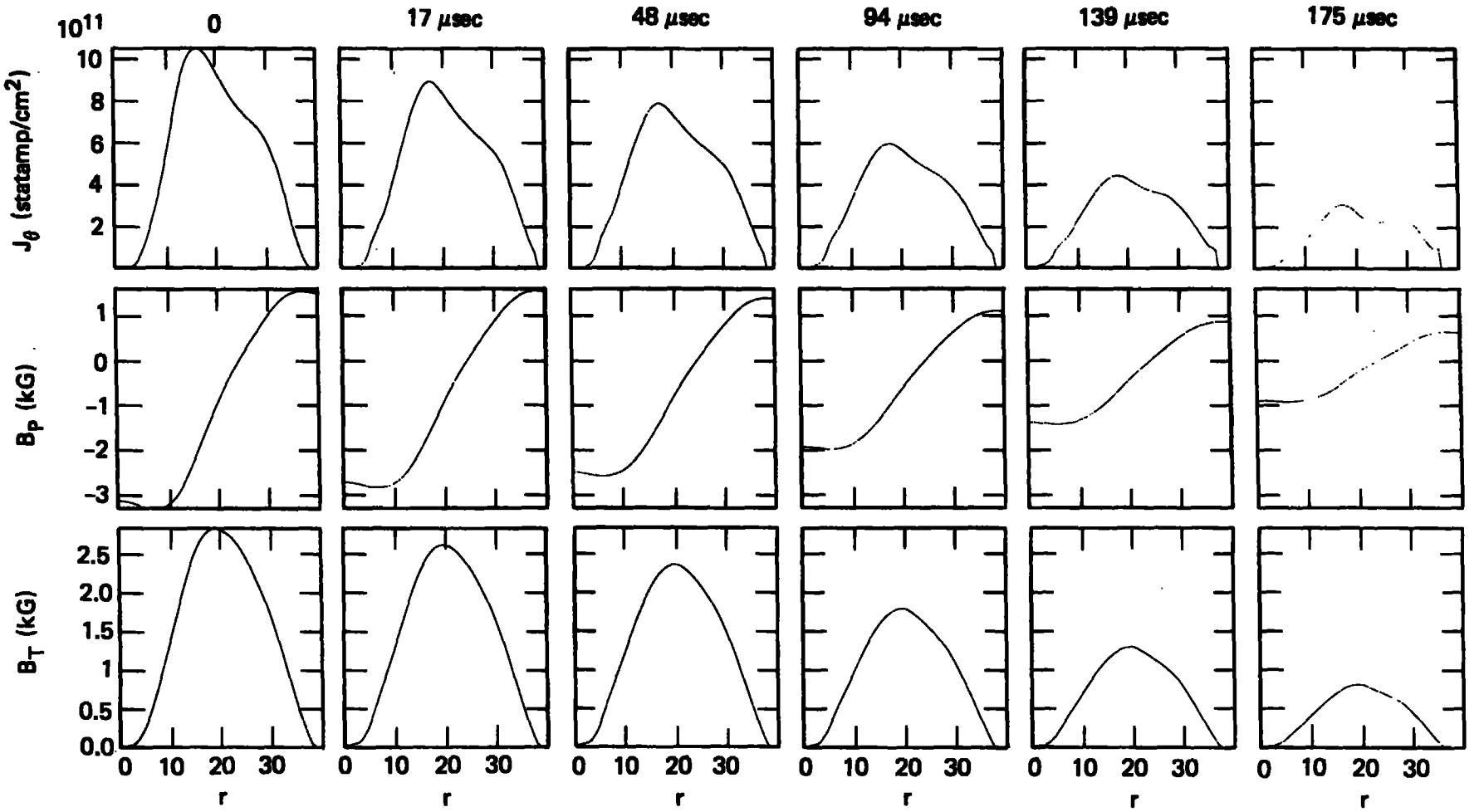
0
17 μsec
48 μsec
94 μsec
139 μsec
175 μsec
10^{11}
J_θ (statamp/cm^2)
B_P (kG)
B_T (kG)
r

Figure 2

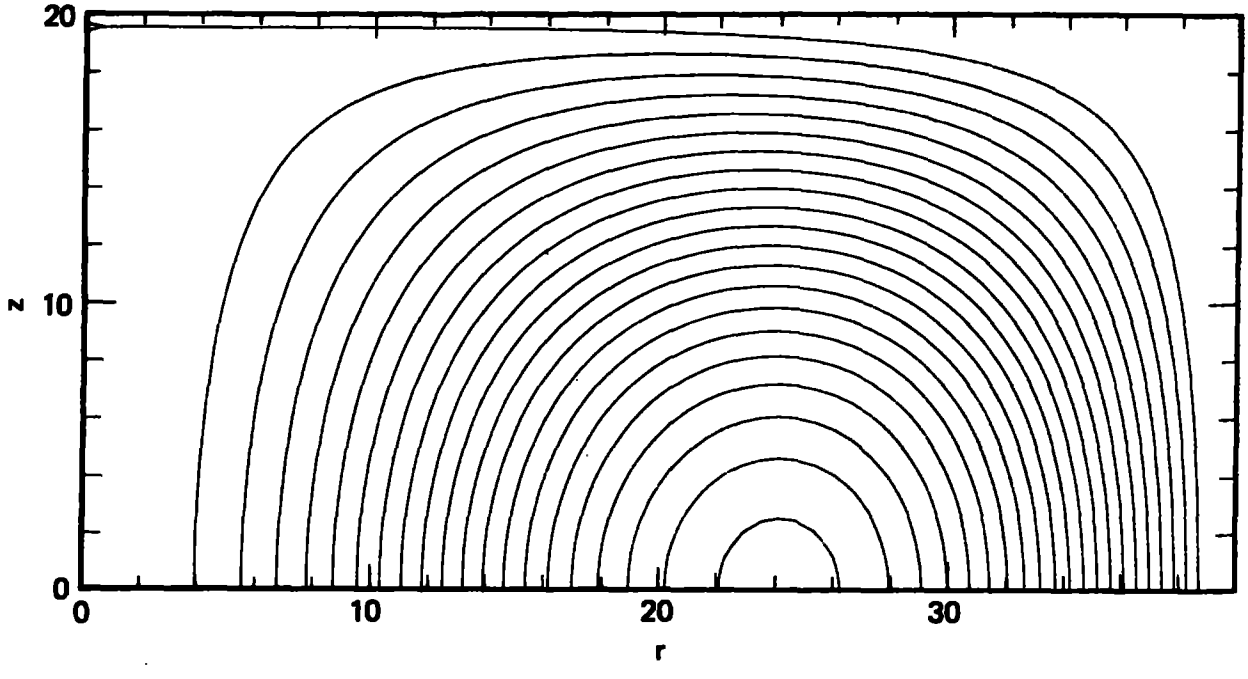

Figure 3

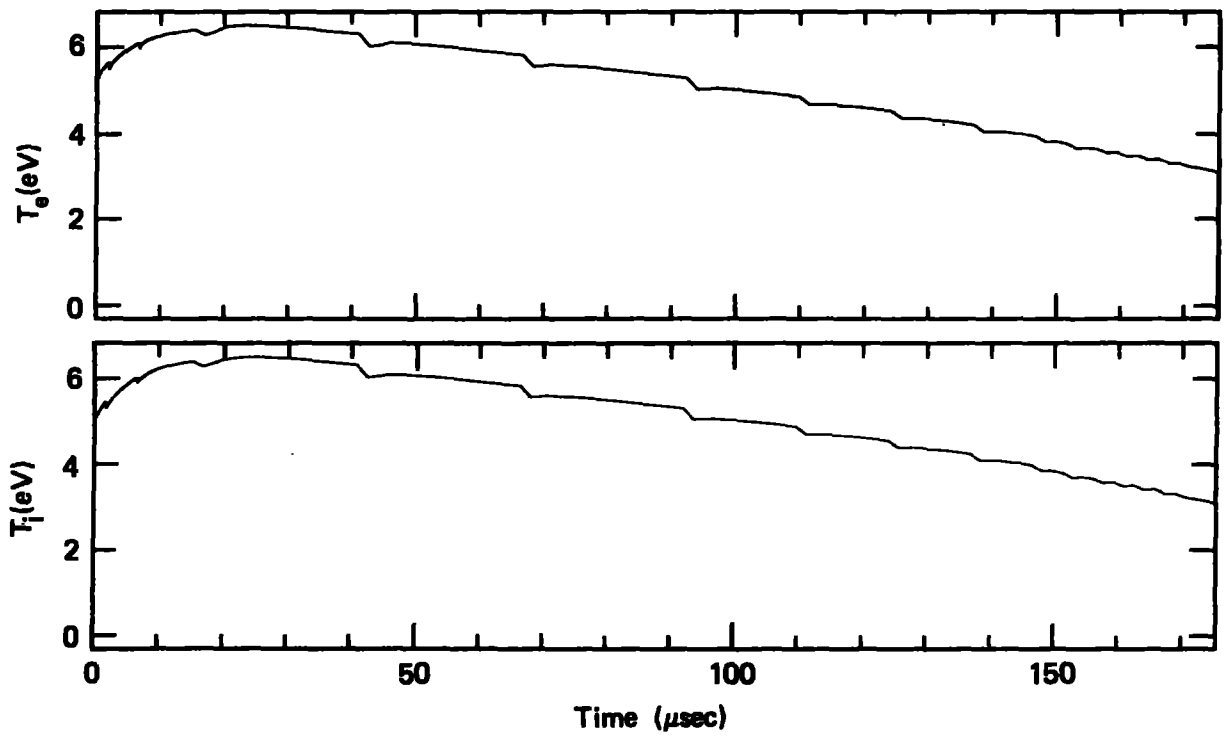

Figure 4

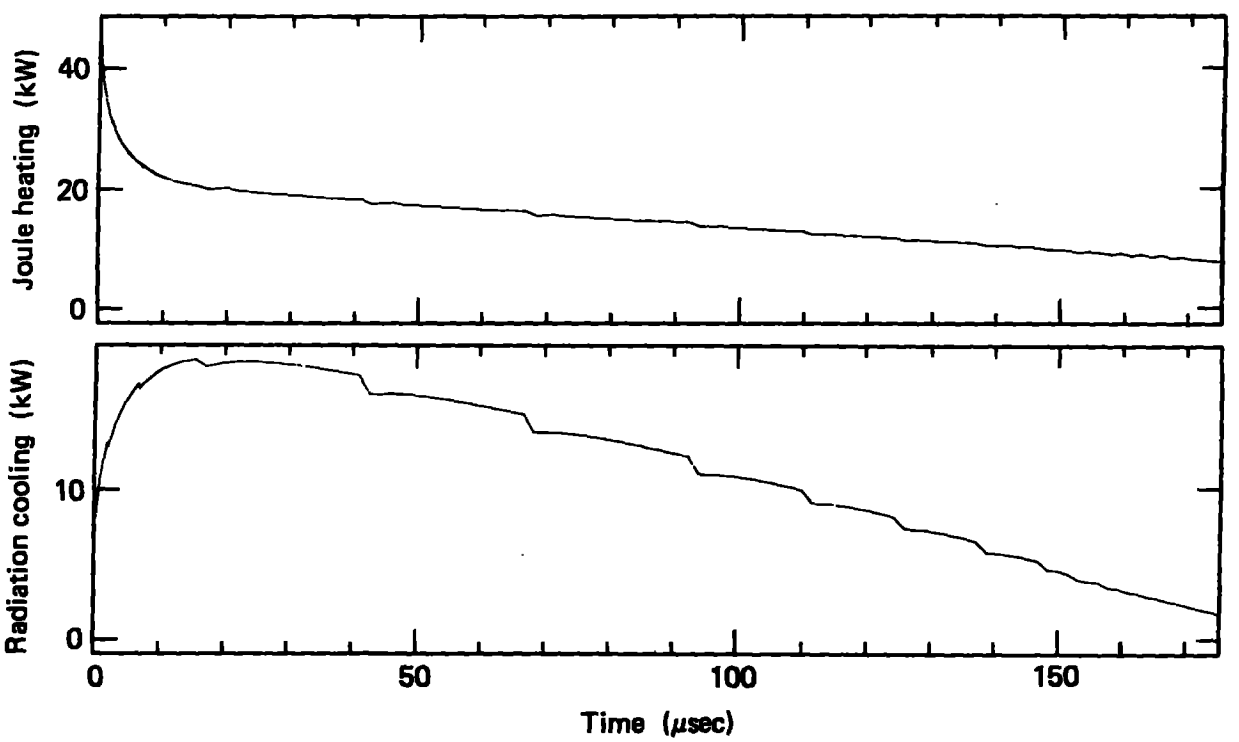
Joule heating (kW)
40
20
0
Radiation cooling (kW)
10
0
0
50
100
150
Time (μsec)

Figure 5

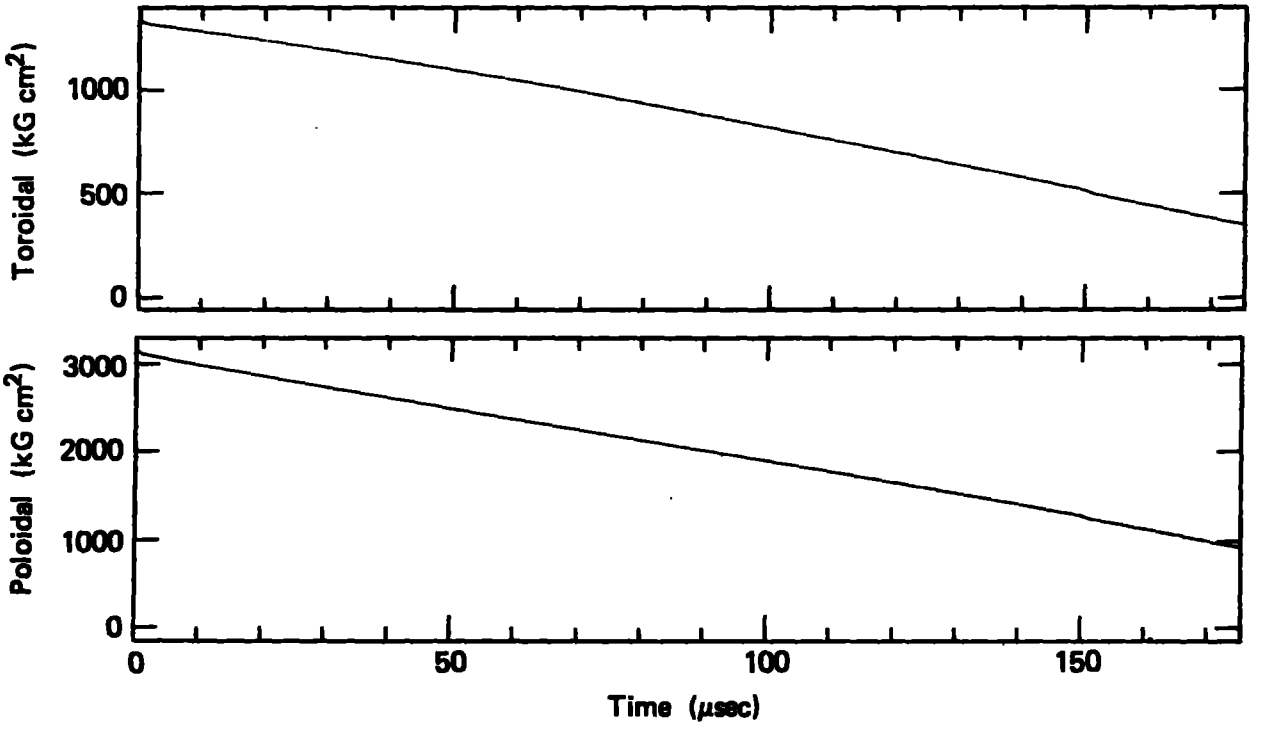
Toroidal (kG cm²)
1000
500
0
Poloidal (kG cm²)
3000
2000
1000
0
0
50
100
150
Time (μsec)

Figure 6

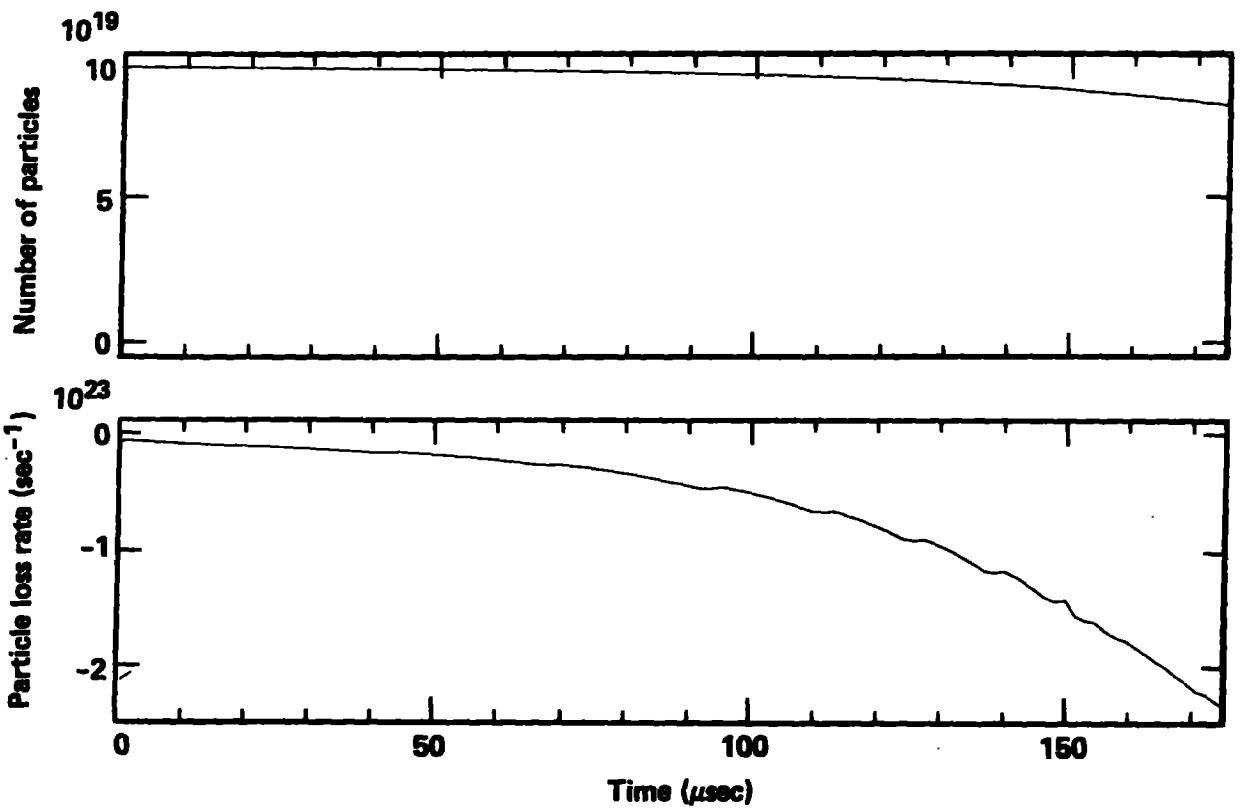
10^{19}
10
5
0
Number of particles
10^{23}
0
-1
-2
Particle loss rate (sec^{-1})
0
50
100
150
Time (μsec)

Figure 7

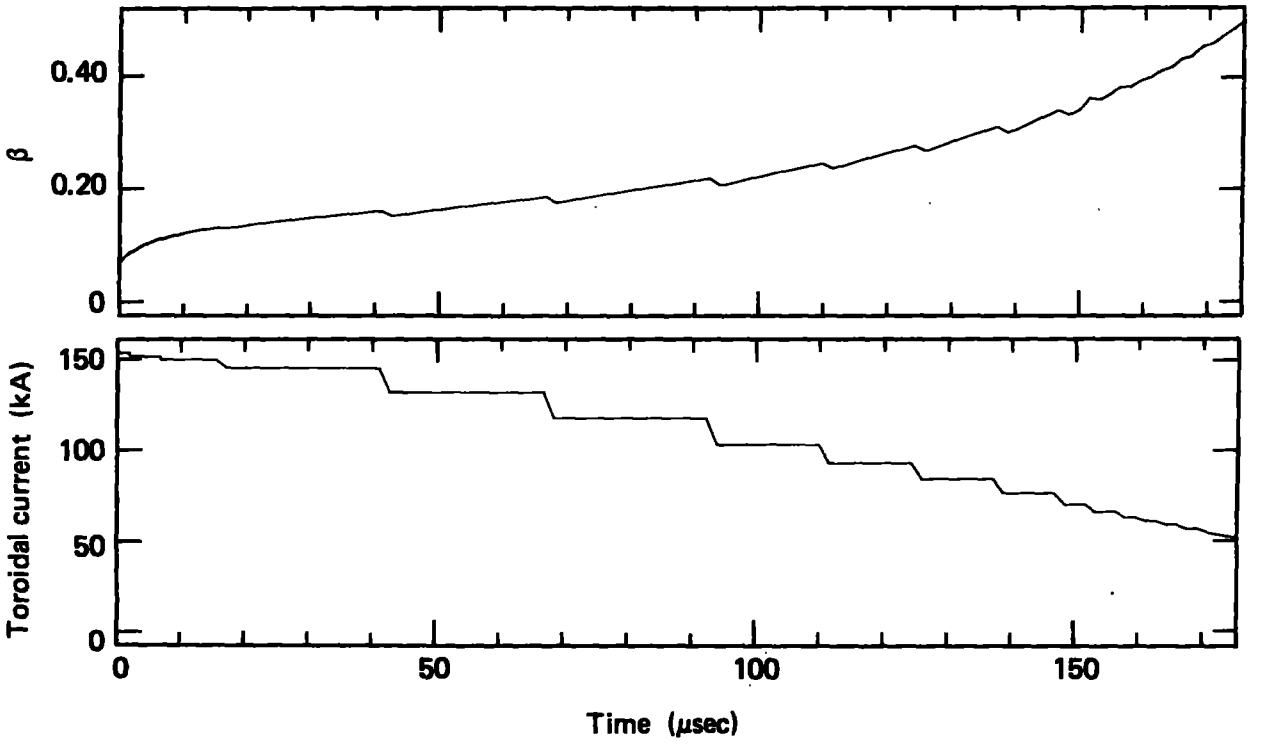
0.40
0.20
0
β
150
100
50
0
Toroidal current (kA)
0
50
100
150
Time (μsec)

Figure 8

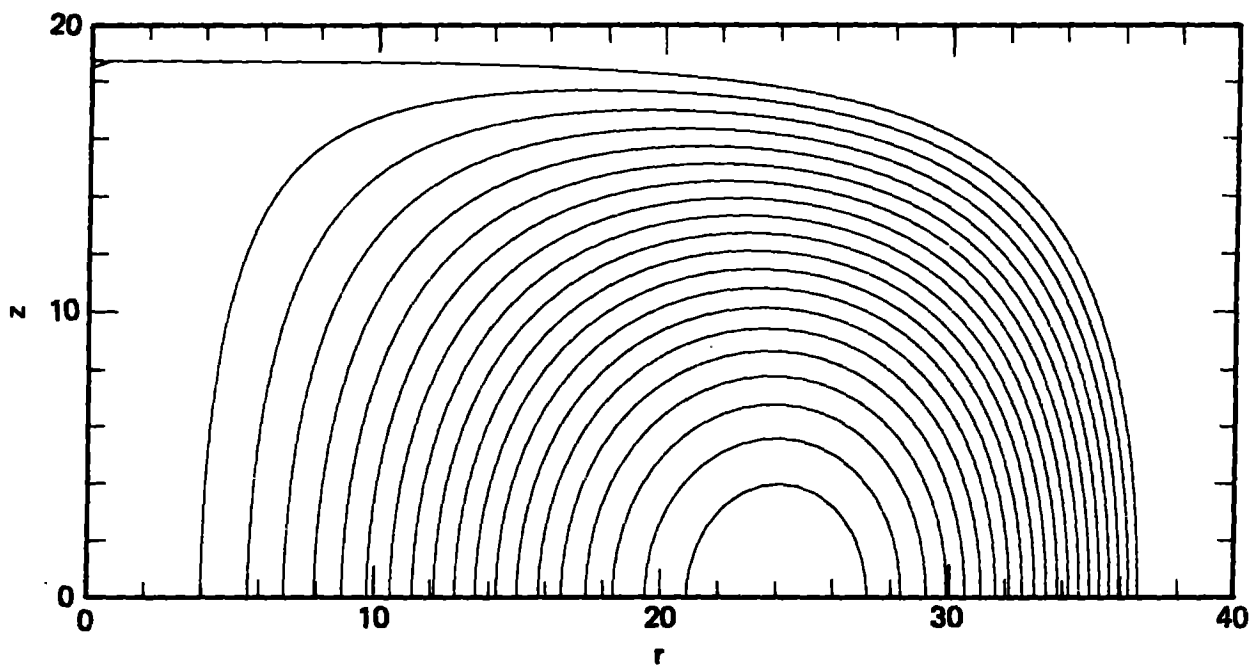

Figure 9